A DFT study of the CO oxidation on the Au(321) surface

José L. C. Fajín[†], *M. Natália D. S. Cordeiro* [‡] *and José R. B. Gomes*[†,§,*]

[†]CIQ-UP and [‡]REQUIMTE, Faculdade de Ciências, Universidade do Porto, P-4169-007 Porto, Portugal

[§]CICECO, Departamento de Química, Universidade de Aveiro, 3810-193 Aveiro, Portugal

*Corresponding Author. E-mail: jrgomes@ua.pt. Phone: +351 234 372 571. Fax: +351 234 370 004

Abstract

The CO oxidation on the Au(321) surface was investigated using spin polarized density functional theory based calculations within the GGA-PW91 exchange-correlation functional. This was done by studying separately the adsorption of isolated CO or CO_2 and also the co-adsorption of CO+O or CO+O_2 on the Au(321) surface. A periodic supercell approach was used to model the gold surface. The kinetic profile of the oxidation reaction was determined with the climbing image-nudged elastic band method and also with the dimer approach. It was found that CO adsorbs on the clean surface preferably at the kinks and the same preference exists if atomic or molecular oxygen is co-adsorbed on the Au(321) surface. Carbon dioxide is weakly adsorbed on Au(321) and appears at large distance from the metal surface. Importantly, the formation of carbonate species or of four atoms compounds, OCOO, adsorbed on the Au(321) surface is thermodynamically favorable from CO and O_2. The reaction of CO oxidation by atomic oxygen occurs almost without any energy cost on a reconstructed surface whereas moderate barriers of ~0.6 eV were computed for the direct reaction with molecular oxygen occurring at the surface steps. These results suggest that the pre-dissociation of the molecular oxygen on the Au(321) surface for the CO oxidation is energetically less favorable than the direct reaction with molecular oxygen. Finally, the products of the oxidation reaction are much more stable than the four atoms compound.

1. Introduction

The discovery in the late nineteen-eighties that highly dispersed gold nanoparticles on a transition metal oxide support catalyzed the oxidation of carbon monoxide at temperatures as low as -70 ºC,[1] lead to a high number of investigations devoted to the understanding of catalysis on gold nanoparticles. The majority of these studies concerned the oxidation of carbon monoxide due to interesting practical applications. These can be either the development of CO sensors[2] or of optimized direct methanol fuel cells (DMFC). In DMFCs, CO appears as an intermediary that inhibits methanol oxidation catalyzed by a Pt-Ru/C substrate and, very recently, its elimination from the catalyst was successfully attained by the addition of gold nanoparticles.[3-4] Recently, gold clusters and gold nanoparticles deposited on more complex supports, such as modernite, showed a significant catalytic activity at low and high temperatures in the oxidation of CO.[5] Gold cations were found to be inactive and its content diminished with the increase of treatment temperature.[5]

Unsupported gold may exhibit high catalytic activity for CO oxidation depending on its intrinsic structure, i.e., depending on the number and size of pores at a nanometer scale yielding a three-dimensional spongy morphology and it seems unlikely to be due to the presence of a support.[6-9] These active gold structures may be either gold-nanotube membranes[6] or nanoporous gold structures.[7-9] Therefore, it is possible to assume that the activity of gold seems to be due to the irregularities of the metal particles or films, which is supported by recent experimental work due to Chen and Goodman.[10] These authors studied the effect of a gold bilayer on a reduced titanium surface also on the reaction of CO oxidation and found that its catalytic activity was comparable to the activity of gold nanoparticles. The exposed surface of the $Au/TiO_2(110)$ catalyst follows the irregularity of the clean $TiO_2(110)$ surface and so it includes a series of steps and kinks, which seems to be the cause for the enhanced activity of some specific gold structures. Contrasting with the assumption introduced above, Schubert et al.[11] studied the effect of different supports on the activity of dispersed gold nanoparticles for CO oxidation. They concluded that the catalytic activity was associated with the reducibility of the oxide supports, i.e., Au catalysts supported on reducible transition metal oxides such as Fe_2O_3 exhibited an enhanced activity for CO oxidation while Au/SiO_2, Au/Al_2O_3 or Au/MgO catalysts were less active. Nevertheless, the same authors found that gold nanoparticles dispersed above an irreducible metal oxide can be active for the reaction of CO oxidation

if the gold nanoparticles are highly dispersed, thus supporting the assumption made above and suggesting a high dependence with the gold morphology.[11] However, the best example of how far we are from a clear understanding of which are the causes for the enhanced activity of some gold catalysts while other are inert for CO oxidation is well documented with two very recent works. Grzybowska-Świerkosz states that the activity of a support should be related with its reducibility,[12] but this is questioned by Comotti *et al.*[13], which showed that gold deposited on Al_2O_3 (irreducible oxide) can be considerable active for CO oxidation while when it is deposited on ZnO (reducible oxide) the activity for the same reaction is poor.

Therefore, it is not surprising that there is a large number of very recent works regarding the understanding of the role of the support and factors that may affect catalysis by gold. Several of these works show the crucial importance of the particle size, and, consequently, of the concentration of low coordinated gold atoms in the catalyst, in the enhancement of the catalytic activity.[14,15] It was found that the support relative surface area is more important than its chemical composition[16] or that the different activities of gold-reducible and gold-irreducible supported catalysts can be explained by the different gold geometries in those catalysts.[17] Other works show that the supports may have a direct influence in the catalytic reaction. For example, nanocrystalline CeO_2 acts as a source of oxygen and also as an oxygen stabilizer,[18] the Au/ZrO_2 interface is the preferential site for molecular oxygen adsorption,[19] the Ti rows of the TiO_2 oxide are the preferential diffusion paths for the migration of oxygen into the gold phase,[20] or the Au_8/MgO(without defects) is less active than the Au_8/MgO(with defects).[21] Other factors, like strain effects due to the mismatch at the gold-support interface,[22,23] the atmosphere gases in contact with the catalyst,[24,25] or the formation of species like carbonates, carboxylates and bicarbonates,[26,27] alter the catalytic activity too.

The catalytic activity is also affected indirectly by the temperature at which the catalyst is calcinated.[28] Wang *et al.*[29] observed the effect of the temperature of calcination on the activity of the Au/SnO_2 catalyst and concluded that the optimum temperature is 300 ºC; the addition of phosphate to the Au/TiO_2 catalyst prevents its deactivation at high temperatures.[30] The role of the charge of gold species was also analyzed: metallic gold is the most important active species in Au/TiO_2,[31] and in Au/CeO_2 catalysts[32]; cationic $Au^{\delta+}$ or $[Au(CO)_2]^+$ gold species were also found in the cases of Au/TiO_2[33], Au/MgO,[34] and Au/CeO_2,[35-37] catalysts and are thought to be active *per se* or by modifying the structure

of the gold particles; trace amounts of anionic species, such as AuO^-, AuO_2^- and $AuOH^-$, were detected when the support was γ–Al_2O_3 or TiO_2 and suggested to have implication in the nature of the active sites of supported Au catalysts.[38] Finally, the catalytic activity can be changed by the addition of other oxides to the catalyst, like BaO in the Au/Al_2O_3 catalyst,[39] or by the addition of other active metals like platinum.[40]

The reaction mechanism concerning CO oxidation by gold has been also extensively studied. In the simplest situations, i.e., in the presence of only CO, O_2 or O species, two different routes are possible, i) reaction with molecular oxygen forming a four atoms (O_2 + CO) transition state or ii) reaction with atomic oxygen, yielding in both cases the desired product, i.e., CO_2. If water is present on the surface, the reaction mechanism may be of even higher complexity.[41]

Liu *et al.*[42] studied the reaction mechanism using spin-polarized density functional theory, DFT, within the generalized-gradient approximation, GGA-PBE, and ultrasoft pseudopotentials, and considering several different Au surfaces, namely, Au(111), Au(211) and Au(221). They found that the latter had the lowest electronic energetic barriers for CO oxidation. In the most reactive Au(221) surface, the most favorable paths for the reaction of carbon monoxide with atomic oxygen or with molecular oxygen at the steps have electronic barriers of 0.25 eV and 0.59 eV (0.46 at high CO coverage), respectively. The energy required to dissociate molecular oxygen yielding adsorbed oxygen atoms is 1.16 eV on Au(221). This value may be compared with the calculated values for the Au(211), 0.93 eV, and Au(111), 2.23 eV, surfaces almost suggesting that dissociation of molecular oxygen is practically unfeasible in the case of the planar Au(111) surface. Importantly, the calculations performed for CO reaction with O_2 on Au(211) or Au(221) surfaces showed a four atoms metastable state. Interestingly, the electronic energy barrier needed to obtain the metastable state is higher than that needed to form the products of the reaction, $CO_{2,g}$ + O_{ads}, from the metastable state.

Lopez and Nørskov[43] used the RPBE exchange-correlation functional and ultrasoft pseudopotentials to investigate the CO oxidation by a gold nanoparticle adsorbed on Ti(110). They considered an isolated Au_{10} cluster as the model of the system and, despite its simplicity, they extracted valuable information. The electronic energy barriers calculated for the reactions with atomic and molecular oxygen are lower than 0.4 eV suggesting that CO oxidation will be possible below room temperature. Furthermore,

they concluded that the main factor for the enhanced activity of the gold particle when compared with other previously studied Au surfaces was the increased number of low coordinated Au atoms associated with a large fraction of corner sites. More recently, Wang *et al*.[44] based on the GGA-PW91 approach and considering a plane-wave basis set, studied two Au_{32} clusters presenting different symmetry and suggested that five-coordinated sites should be more active than six-coordinated sites. Furthermore, they suggest also that small molecules should be adsorbed more favorably on the former than on the latter sites. The calculated electronic adsorption energies for CO, H_2 and O_2 were more favorable in the case of the less symmetric Au_{32} cluster studied.

The influence of several different faces of the ZrO_2 support on CO oxidation by gold has been studied very recently by Wang et al.[19] GGA-PBE/DZP calculations were performed on both monoclinic and tetragonal phases of the ZrO_2 support, namely, the flat m-$ZrO_2\{\bar{1}11\}$ and t-$ZrO_2\{101\}$ surfaces and the stepped m-$ZrO_2\{\bar{2}12\}$, and t-$ZrO_2\{302\}$ ones. They found that molecular oxygen is adsorbed in the interphase between a gold strip with 2 atomic layers and the ZrO_2 support. The maximum electronic adsorption energy found is 1.71 eV for the stepped t-$ZrO_2\{302\}$ support. The adsorption of CO was more favorable on low coordinated gold atoms, in agreement with the results due to Lopez and Nørskov.[43] Similarly to previous results calculated for CO oxidation on unsupported Au surfaces,[42] a metastable state was found when carbon monoxide reacts with molecular oxygen above Au/ZrO_2 catalysts; the relative electronic energy barriers between the initial and the metastable states and between the metastable state and the products depend on the phase and on the face of the ZrO_2 support. The largest electronic barriers are found when the Au strip is deposited on the flat m-$ZrO_2\{\bar{1}11\}$ surface, values of 0.63 and 0.39 eV, respectively. In the other three cases, the complete reaction yielding gaseous carbon dioxide and adsorbed atomic oxygen needs to surmount a maximum electronic barrier of ~ 0.3 eV, a value that is not far from that calculated by Lopez and Nørskov on different gold scaffold and oxide.[43]

Another important aspect in the CO oxidation reaction is the form how oxygen is deposited on the surface.[45-47] Several different forms of oxygen deposited on gold surfaces were found. For example, Min *et al*.[47] identified the following species on Au(111): chemisorbed oxygen, surface gold oxide or bulk gold oxide. These different forms of deposited oxygen are characterized by different reactivities towards CO oxidation. Chemisorbed oxygen was identified as the most active species concerning CO

oxidation while the bulk oxide is the least reactive. It was found also that the type of deposited species depended on both the temperature and oxygen coverage. The highest rate of CO oxidation was observed for an initial oxygen coverage of 0.5 monolayers deposited at 200 K, for which the density of chemisorbed oxygen is maximized.

Very recently, we have studied by means of periodic GGA-PW91/plane-wave calculations, the effects on the structure of Au(321) caused by consecutive deposition of oxygen atoms on that stepped gold surface.[48,49] Our calculations showed that oxygen atoms are strongly adsorbed on the Au(321) surface or even under the outermost gold layer, causing strong reconstruction and generating either planar or stepped surfaces.[48] The calculations showed also that formation of differently coordinated oxygen species are thermodynamically favorable with respect to the energies of gaseous molecular oxygen and of the clean metal surface. This enhanced stability seems to be correlated with the large number of low-coordinated Au atoms. The dissociation of molecular oxygen on the Au(321) surface was also studied. In the most favorable case, i.e., dissociation occurring at the steps of the Au(321) surface, the calculated electronic energy barrier was 1.00 eV.[49]

From what has been written above, there are still many questions regarding the unique catalytic properties of gold containing catalysts. It seems that the most important factor is linked with the type of the metallic particles or films, more precisely, on the neighborhood of the exposed gold atoms. Low-coordinated gold atoms seem to be much more active than highly-coordinated ones.[19,43,50] The stepped Au(321) surface has many low-coordinated atoms due to its *zig-zag* step line. It presents several corner sites that were suggested to be important catalytic centers[43] and that are absent in other stepped surfaces studied previously. Thus, this surface seems to be a good model to study the influence of the low-coordinated atoms in catalysis by gold since it includes a rather high heterogeneity of adsorption sites, i.e., surface positions in the middle of terraces, nearby kinks or steps, resembling more a real catalyst than other surfaces with lower Miller-indices.

This work is focused on the reaction of CO oxidation on the Au(321) surface and it is intended to be a contribution for a better understanding of the catalytic properties of gold surfaces. It is organized as follows. The computational methods are described in detail in section 2 while the calculated results are reported and discussed in section 3. Finally, the most important conclusions are summarized in section 4.

2. Computational details

2.1. *DFT approach.*

The VASP 4.6.3 computer code[51] and the GGA-PW91 functional proposed by Perdew *et al.*[52] were used to carry out the density functional theory calculations. The projected augmented-wave (PAW) method due to Blöch[53] and further implemented by Kresse and Joubert[54] was employed to describe the effect of core electrons on the valence shells together with a plane-wave basis set used to span the valence electronic states. Several tests were done for the adsorption of CO on the Au(321) surface and a cutoff of 415 eV was found to be sufficient for reaching convergence on both energies and geometrical parameters. During the spin-polarized calculations, the positions of the ions were relaxed using the conjugate-gradient algorithm. The Monkhorst-Pack k-points grid used was 5x5x1 which has been tested in a previous work.[49] The electronic energetic barriers for carbon monoxide reaction with molecular and atomic oxygen were obtained using the *climbing-image nudged elastic band* (cNEB) method.[55,56] In some cases, the dimer method[57] has been used in the location of TS structures or to further refine the structures obtained until the force on the optimized ions dropped below 0.005 eV/Å. The computation of a single imaginary frequency ensured that the structures located with the cNEB and dimer approaches were true transition states.

The PW91 functional has been used throughout this work but the reader should be aware that energies calculated with this exchange-correlation functional may differ significantly from those obtained with other exchange-correlation functionals.[58] Furthermore, comparison with results from previous works[19,42-44] needs some additional caution since other parameters introduced in the computations, c.f., cut-off, pseudopotentials, etc., may be also different.

2.2. Slab model

We used the three-dimension (3D) periodic-slab approach for the representation of the infinite Au(321) surface and of the interactions of this surface with isolated CO and CO_2 molecules and also with molecular or atomic oxygen co-adsorbed with CO or CO_2. The positions of the gold atoms in the stepped Au(321) surface were optimized in a

previous work.[49] Fifteen gold atoms were used to model a four-layer slab corresponding to the (321) Miller index. A vacuum region of 10 Å thick was introduced between repeated cells in the *z* direction in order to build a surface. During the calculations, the uppermost seven gold atoms have been fully relaxed while the other eight were kept frozen. According to the notation proposed by McFadden *et al.*[59], the uppermost relaxed surface with which the adsorbents were allowed to interact is the Au(321)^S face. The unit cells consist of a monoclinic prism with the angle between the *x* and *y* axis being different from 90 degrees and the two other involving the *xz* and *yz* axis of exactly 90 degrees. Further, in this crystal system, the vectors *x*, *y* and *z* have different lengths with Au-Au bond distances being of 2.9161 Å. The stepped Au(321) surface has a large variety of possible adsorption positions, as shown in Figure 1. The different possible hollow sites are labeled in Figure 1 with *a*, *b*, *c*, *d*, *e*, *f*, *g*, *h* and *i* letters while the top sites are labeled with *1*, *2*, *3* and *4* numbers. The different bridge positions are not illustrated in Figure 1 but are, from now on, labeled with the letter *b* followed by the numbers of the two nearest-neighbor gold atoms, ordered with respect to the view from the right to the left and from the positions closer to the reader to those farther.

3. Results and discussion

The adsorption of atomic and molecular oxygen on the Au(321) surface was studied in a previous work[49] aiming the determination of the most favorable adsorption positions as well as the energetics regarding O_2 dissociation on the metallic surface. Atomic oxygen is preferentially adsorbed on a *fcc* hollow site nearby the step, labeled as hole "*a*" in Figure 1, with an adsorption energy of -0.16 eV calculated with respect to the clean slab and gas-phase molecular oxygen. All the other adsorption positions have positive energies and, hence, are unfavorable. The most stable adsorption position for molecular oxygen corresponds to a configuration with the molecular axis parallel to the (111) terrace and aligned with one of the bridge sites in the steps of the Au(321) surface ($b_{1\text{-}2}$ in Figure 1). This configuration was found to be more favorable than the separated fragments by -0.17 eV. In the most favorable path for molecular oxygen dissociation, the O-O bond is cleaved nearby the step with one oxygen atom remaining in the upper (111) terrace (site "*d*" in Figure 1) while the other is adsorbed on the step (site "*h*" in Figure 1). The calculated electronic energy barrier for O_2 dissociation on the Au(321) surface was

1.00 eV, much less than that computed for Au(111), 2.23 eV,[42] suggesting that the former is much more active.

In this work, the adsorption of CO and CO_2 on the same Au(321) surface was studied. The adsorption energies on the different sites shown in Figure 1 were calculated as:

$$E_{\text{ads,CO}} = E_{\text{slab–CO}} - E_{\text{slab}} - E_{\text{CO}} , \quad (1)$$

$$E_{\text{ads,CO}_2} = E_{\text{slab–CO}_2} - E_{\text{slab}} - E_{\text{CO}_2} . \quad (2)$$

Furthermore, it was also studied the co-adsorption of CO with atomic or with molecular oxygen on Au(321). The energies of co-adsorption were calculated as:

$$E_{\text{coads,CO+O}} = E_{\text{slab–(CO+O)}} - E_{\text{slab}} - E_{\text{CO}} - \frac{1}{2} E_{\text{O}_2} , \quad (3)$$

$$E_{\text{coads,CO+O}_2} = E_{\text{slab–(CO+O}_2\text{)}} - E_{\text{slab}} - E_{\text{CO}} - E_{\text{O}_2} . \quad (4)$$

In the equations above, the first term corresponds to the energy of the adsorbate-surface supermolecule. The other terms, E_{slab}, E_{CO}, E_{CO2}, and E_{O2}, correspond to the energies of the clean Au(321) surface and of gaseous CO, CO_2 and O_2, respectively. Therefore, negative values of E_{ads} (E_{coads}) mean favorable adsorption (co-adsorption) energies. In the coming sub-sections it will be presented and discussed the results concerning the adsorption of CO and CO_2 on the Au(321) surface as well as the results calculated for the CO molecule co-adsorbed and reacting with atomic or molecular oxygen.

3.1. Adsorption of CO

The interaction of the C-down carbon monoxide molecule with the Au(321) surface has been considered for all the sites shown in Figure 1. The optimal distances and the calculated energies with respect to the separated fragments are given in the Supporting Information while those corresponding to adsorption on the most favorable sites are summarized in Table 1.

The preferred site for CO adsorption is on top of the gold atoms on the edges of the (111) terraces, i.e., those with labels "*1*" in Figure 1. The calculated interaction energy is -0.77 eV and the C-Au distance is 1.97 Å. The final optimized structure is

shown in Figure 2a. On the other top sites considered, adsorption is less stable than that occurring above atom "*1*". Furthermore, CO adsorption on top of atoms "*2"* and "*3"* is also less favorable than on some bridge and three-hollow sites. In the case of positions "*4*" and "*5*", CO adsorption is found to be unstable and upon the optimization procedure, the CO molecule ends interacting with atom "*1*".

In the cases of the bridge sites connecting atoms "*1*" and "*2*", the calculated interaction energies are approximately -0.6 eV and the C-Au distances are ~2.1 Å. Interestingly, the three-hollow sites where atom "*1*" appears in one of the corners, i.e., sites "*a*", "*b*" and "*g*" shown in Figure 1, are more stable than the other top and bridge sites considered where "*1*" is not present. This suggests that on the Au(321) surface, the low coordinated gold atoms at the edges of the (111) terraces have an important role in the stabilization of the adsorbed CO molecule. Adsorption on hollow sites "*h*" and "*i*" was not found since the CO molecule prefers to be attached to atom "*1*"and to hollow "*f*", respectively.

The C-O distance for adsorption on top is 1.15 Å and it changes to 1.17 Å in the cases of the bridge and hole sites. This variation of the C-O distance was also observed in previous works dealing with CO adsorption on gold clusters.[40,44]

Finally, the adsorption of carbon monoxide on top sites but in O-down orientation was also studied but it was found to be always unfavorable (results given in the Supporting Information).

3.2. Adsorption of CO_2

In the present work, the adsorption of carbon dioxide was studied both for the molecule with its axis normal or parallel with respect to the Au(111) terraces on the Au(321) surface. The most stable configuration obtained from the several starting geometries considered (seven hollow, nine bridge and four top sites with data compiled in the Supporting Information) is depicted in Figure 2b. As expected, the most important conclusion is that CO_2 interacts weakly with the Au(321) surface and, so, computed interaction energies with respect to the separated fragments are approximately zero. Consequently, the adsorbate to surface distances are large and the C-O bond lengths are equal to those calculated for gaseous CO_2. Thus, if carbon dioxide is formed on the surface it will desorb easily.[60] However, if the interaction energy is calculated with respect to the energies of CO and one-half of O_2, in the gas-phase, the values of the

adsorption energies are in the range -3.2 eV to -3.3 eV. These values are 0.4 eV less negative than the RPBE interaction energy reported by Remediakis et al.[15] for CO_2 adsorption on an Au_{10} cluster supported on TiO_2.

3.3. Co-adsorption of CO and O

Considering that CO is preferentially adsorbed on sites closer to the step and in C-down orientation, the study of the CO and O coadsorption was carried out by placing one CO molecule and one oxygen atom per unit cell on several different possible positions on the Au(321) surface. We found previously that the introduction of several adsorbed species on the Au(321) surface may lead to strong reconstructions of the surface and that these are only possible to be ascertained if several different starting positions are considered.[48] Therefore, in the present study, 57 different initial positions for O+CO co-adsorbed on the Au(321) surface were idealized. From these initial configurations, 34 different structures where CO and O species appear on the surface were obtained. In the other 23 cases, some configurations lead to formation of CO_2 (O,CO: hole "*b*", b_{3-2}; hole "*b*", hole "*a*"; hole "*a*", hole "*c*"; hole "*a*", top "*2*"; hole "*a*", b_{1-2}; hole "*b*", top "*2*"; hole "*b*", b_{2-1}; hole "*h*", b_{1-2}; and hole "*h*", hole "*f*") while some other were optimized to the same final states obtained with different initial configurations. Energetic and structural data of selected configurations are reported in Table 2. Detailed results concerning the other configurations studied may be found in the Supporting Information.

The most favorable configurations optimized for CO and O co-adsorbed on the Au(321) surface are characterized by the interaction of atomic oxygen and of the CO molecule with the surface atom "*1"*. These simultaneous interactions produce strong surface relaxation around atom "*1"*. For example, in the case of O and CO co-adsorbed on the hole "*b*" and top "*1*" sites, respectively, the interaction leads to an important elongation of the bond between surface atoms "*2"* and "*1"*. For O and CO co-adsorption on hole "*h*" and top "*1*" or on hole "*g*"- top "*1*" positions, the bond between atoms "*4"* and "*1"* is strongly enlarged. The final optimized structures for these three cases have interaction energies of -1.03 eV, -0.84 eV and -0.82 eV and are shown in Figures 3a, 3b and 3c, respectively. When these structures are compared with those where co-adsorption is not accompanied by surface deformation, the optimized O-Au and C-Au distances decrease from typical values of 2.0-2.2 Å to values of 2.0 Å for atomic oxygen and 1.9 Å for carbon monoxide. These shorter adsorbate to surface distances accompanied by larger

interaction energies similar to the results obtained previously when two oxygen atoms are co-adsorbed on the Au(321) surface.[49] In the most favorable situation, the present PW91 co-adsorption energy is approximately 0.4 eV more negative than the RPBE value reported by Remediakis et al.[15] for CO and O co-adsorption on a Au_{10} cluster supported on a TiO_2(110) substrate.

Within the configurations without surface deformation, the most favorable situation (Figure 3d) is that where O and CO species are co-adsorbed on hole "*d*" and top "*1*" sites, respectively. The calculated adsorption energy is -0.72 eV, the C-Au distance is 1.96 Å and the distance between the adsorbed oxygen atom and the nearest surface atom "*2*" is 2.15 Å.

An inspection of the other configurations with CO and O co-adsorbed on the surface shows that the most favorable are those with CO adsorbed atop atom "*1*" or located at the edge of the (111) terrace, showing the importance of steps, or other surface irregularities with low-coordinated Au atoms, in the adsorption of CO and consequently, in the oxidation of CO by atomic oxygen. Finally, the optimized CO distances are identical to those reported in sub-section 3.1., i.e., ~1.15 Å if carbon monoxide is adsorbed on top of gold atoms and it varies between 1.16-1.17 Å if it is adsorbed on bridge or hollow sites.

3.4. Co-adsorption of CO and O_2

Thirty different initial configurations for carbon monoxide and molecular oxygen co-adsorbed on the Au(321) surface were considered. Knowing that the oxygen molecule is adsorbed weakly on this gold surface,[49] and that CO is preferentially adsorbed at the edges of the (111) terraces, the selected configurations benefit the higher adsorption energy of the latter, i.e., they have the CO molecule positioned nearby the minimum in the potential energy surface. Some of the initial configurations lead to the formation of a carbonate species on the surface or to the formation of a four atoms compound, similar to the peroxy-acetate organic group, adsorbed on the bridges that form the step. Adsorption energies calculated with eq. 4 as well as geometrical details for selected configurations are given in Table 3. Results calculated for all the configurations studied may be found in the Supporting Information.

Since the oxygen molecule is weakly adsorbed on the Au(321) surface, the optimized configurations for co-adsorbed CO and O_2 are 0.25 eV less stable than

adsorbed OCOO and 2.77 eV less stable than adsorbed CO_3 species. The formation of the adsorbed carbonate species, shown in Figure 4c, is explained by its high stability on the Au(321) surface, E_{ads}= -3.53 eV, and also to the fact that the initial positions of the CO and O_2 molecules were too close and destabilizing. It should be noted that it is not meant that the reaction leading to the formation of the adsorbed carbonate species proceeds without energy barrier. During the optimization procedure, the carbon atom of the CO molecule with its axis normal to the terrace and above hole "*a*" interacts directly with the O-O bond of the O_2 molecule placed horizontally on $b_{1\text{-}2}$. This reaction needs the cleavage of the O-O bond which on the steps of the Au(321) surface costs ~1.0 eV but on the (111) terraces is relatively costly, ~2.2 eV.[42,49] This reaction competes with the reaction leading to the formation of CO_2 and this finding is in agreement with the experimental observation of adsorbed carbonate species on the active sites of gold catalysts during CO oxidation[24-27], which was suggested to slow down the reaction of CO oxidation.

The four atoms compound, similar to the peroxy-acetate organic group, adsorbed on the bridges that form the step, is formed without electronic energy barrier if CO and O_2 are already adsorbed on the gold surface. The two configurations obtained are depicted in Figures 4a and 4b. The four atoms compound obtained in this work resembles a metastable state found by Liu and co-workers when studying with the PBE exchange-correlation functional and with the DZP basis set the CO oxidation on stepped Au(211) and Au(221) surfaces and on Au strips deposited on different ZrO_2 supports.[19,42] In the present study, the absence of a transition state structure has been checked by calculations employing the *cNEB* approach. Several possible directions were tested either starting from the adsorbed OCOO species or from CO adsorbed on top "*1"* or top "*2*" sites with the O_2 molecule above neighboring positions. Nevertheless, it should be emphasized here that their transition state structures were obtained for adsorbed CO interacting with gaseous O_2, in the cases of the pure metallic surfaces, and for CO adsorbed on the Au strips interacting with O_2 adsorbed on the oxide support, in the case of supported gold strips. These cases are not exactly the same situations as those we are reporting here.

In the most stable structure optimized for separated CO and O_2 fragments on the Au(321) surface, CO is located 1.99 Å above atom "*1"* and O_2 is placed nearby sites "*2"* and $b_{3\text{-}2}$. The O-Au distances to atoms "*2"* and *"3"* are 2.36 Å and 2.68 Å, respectively, while the O-O distance is 1.28 Å. A deeper analysis of the other less stable optimized configurations which are given as Supporting Information shows that the O_2 molecule is

always weakly adsorbed on the surface with O-O and O-Au distances similar to those obtained in a recent study devoted to the adsorption of O and O_2 species on the same Au(321) surface.[49] The O-O distances vary in the range 1.24-1.30 Å and the O-Au distances are greater than 2.5 Å. The influence of the co-adsorbed O_2 molecule on the geometry of carbon monoxide is negligible and the C-O and C-Au distances have values similar to those reported in sub-section 3.1. The calculated interaction energy for the most stable configuration optimized for co-adsorbed CO and O_2 molecules is -0.76 eV. This value is almost 1 eV less negative than the RPBE energy of co-adsorption computed by Remediakis et al.[15] on a rutile-supported Au_{10} cluster. The larger co-adsorption energy calculated in the case of the supported gold particle is probably due to a stronger interaction between the oxygen molecule and the metal oxide supports, but it may be also influenced by the choice of different DFT approaches.[15,19]

3.5. Reaction profile for the CO oxidation on the Au(321)

Carbon monoxide may suffer oxidation to CO_2 by reaction with an oxygen atom adsorbed on the surface and formed by previous dissociation of molecular oxygen, or by direct reaction with molecular oxygen.[42] Previously, we found that the dissociation of molecular oxygen on the Au(321) surface presents a moderately high energetic electronic barrier of ~1 eV. The energy required to break the O-O bond of molecular oxygen is an obstacle for the CO + O reaction since the preferred dissociation path for the dissociation reaction is nearby the steps which are the places where the CO molecules are also preferentially adsorbed. Therefore, it is possible to suggest that the preference of the CO molecules for such sites “poisons” the catalyst. Nevertheless, the reaction of CO + O_2 producing CO_2 leaves an oxygen atom on the catalyst[60] and, therefore, the adsorbed CO molecules poisons only the reaction of dissociation of O_2 and not the reaction between carbon monoxide and atomic oxygen.

The reaction paths for the reaction between carbon monoxide and atomic oxygen on the Au(321) surface considered as initial structures the configurations shown in Figure 5.

In the configurations with surface deformation, Figures 3a-c, the reaction leading to the production of gaseous carbon dioxide proceeds via the TS structures shown in Figure 5. In the case of the most stable reconstructed configuration, Figure 3a, the

reaction occurs along the $b_{1\text{-}2}$ site with a concomitant decrease of the length of the bridge connecting atoms "*2*" and "*1*" from 3.49 Å to 3.21 Å as shown in Figure 5a. The O---CO and Au---CO distances in the TS are 2.48 Å and 2.05 Å, respectively. Interestingly, the nearest-neighbor Au---O distance is slightly reduced due to the decrease of the number of Au atoms to which the oxygen atom is bonded. The calculated electronic energy barrier from configuration in Figure 3a is 0.75 eV and the imaginary frequency is 48 cm^{-1}. Considering as starting structures the configurations shown in Figures 3b and 3c, the reaction between carbon monoxide and atomic oxygen proceeds via the TS structures shown in Figures 5b and 5c, with calculated electronic energy barriers of 0.01 and 0.02 eV, respectively. These DFT based and ZPE uncorrected energetic differences must be treated with caution. The vibrational frequencies associated with these two TS states are 65 cm^{-1} and 81 cm^{-1}, respectively. The O---CO distances in the initial states are of about 3.0-3.1 Å and are reduced to ~2.4 Å in the TS states. In the three situations above, the reaction of CO with atomic oxygen proceeds with the restoration of the unreconstructed Au(321) surface.

In the case of the reaction of carbon monoxide and atomic oxygen on the slab without surface deformation, i.e., starting from the configuration in Figure 3d, the oxidation reaction proceeds via the structure shown in Figure 5d. The calculated energy barrier is 0.24 eV, with a O---CO distance of 2.38 Å, and the corresponding imaginary frequency is 150 cm^{-1}. The TS structure connecting the configuration shown in Figure 3d and gaseous carbon dioxide above the Au(321) surface resembles the TS structure calculated for the diffusion of atomic oxygen from hollow site *d* to hollow site *b*, for which a electronic energy barrier of 0.48 eV has to be surpassed. Considering the energy of the unreconstructed configuration shown in Fig. 3d, the reaction path leading to the formation of gaseous CO_2 is exothermic by 2.60 eV.

Importantly, from the discussion above, it seems that some structures with intercalated oxygen atoms, e.g., configurations shown in Figures 3b and 3c, are important in the course of the oxidation of CO, by stabilizing the reactants and by lowering the energy barriers. Very recently, the presence of a thin RhO_2 oxide film on the $Pt_{25}Rh_{75}(100)$ surface was found to be related with an increase in CO_2 production in the interface between these regions;[61] Thus, since we have found very recently some very stable configurations with up to 4 intercalated oxygen atoms on the same unit cell used

here to model the Au(321) surface,[48] the role of the intercalated oxygen atoms in the reaction of oxidation of CO is something that we would like to address in the near future.

The direct reaction was studied from OCOO four atoms species adsorbed on the edges of step, i.e., sites $b_{1\text{-}2}$ and $b_{2\text{-}1}$, since these configurations are ~0.3 eV more stable than those with separated CO and O_2 fragments. The reaction of OCOO towards CO_2 and O species occurring on the Au(321) surface is characterized by two similar transition states with electronic energy barriers of 0.56 eV in the case of the site $b_{1\text{-}2}$ and of 0.58 eV in the case of the site $b_{2\text{-}1}$. The computed single imaginary frequencies have values of 842 cm^{-1} and 836 cm^{-1}, respectively. In these transition states, the C-O distance is 1.25-1.26 Å while the O-O distance is 1.77 Å (Figures 6a and 6b). The products of the reaction after the cleavage of the OCO-O bond are shown in Figure 6c. The resulting oxygen atom stays adsorbed on the hollow site "*a*" while the CO_2 molecule appears at a large distance from the metal surface suggesting immediate desorption. Considering the energy of the four atoms compounds and the energy of the final state the reaction is exothermic by 2.44 eV and 2.42 eV for the reaction involving the four atoms compound adsorbed on $b_{1\text{-}2}$ and $b_{2\text{-}1}$ sites respectively. Interestingly, the two reaction paths have similar energetic cost which contrasts with the 0.2 eV difference for the reaction of dissociation of molecular oxygen occurring also on $b_{1\text{-}2}$ and $b_{2\text{-}1}$ sites.[49] A profile of the reaction above the $b_{2\text{-}1}$ site is given in Figure 7.

The calculated electronic energy barrier for the reaction of oxidation on the Au(321) surface is 0.2-0.4 eV higher than the PBE/DZP electronic barriers recently computed on zirconia-supported gold strips.[19] Despite the consideration of different exchange-correlation functionals and basis sets, there are significant differences between the present study and others reported previously either for stepped gold surfaces or for supported gold particles.[19,42] In those works, the formation of the OCOO species from CO and O_2 needs to surmount a larger energy barrier than that calculated for the formation of CO_2 and O from OCOO, with a single-exception, that is for a gold strip adsorbed on the t-ZrO_2{302} support. In the latter case, the energy required to form the four atom species from carbon monoxide and molecular oxygen is only 0.08 eV while that for the cleavage of the OCO-O bond needs 0.33 eV. For example, on the other studied stepped gold surfaces, the oxidation of CO on the Au(211) and on the Au(221) surfaces by direct reaction with O_2 and producing the metastable OCOO state has energy barriers of 0.68 eV and 0.59 eV, respectively, while the dissociation of the OCOO

species towards the CO_2 + O products has barriers of 0.43 eV and 0.42 eV, respectively.[42]

3.6. Analysis of the electronic structure during CO oxidation

The electronic structures of the adsorbed species and of the surface atoms "*1*" and "*2*" were analyzed for several selected stationary points thought to be important for the elucidation of the reaction of CO oxidation on the Au(321) surface. The analysis of the projected density of states (p-DOS) was performed for the most stable configurations on the Au(321) surface of CO and CO_2, of co-adsorbed CO and O species and also of the four atoms compound.

The p-DOS for the free CO molecule is shown in panel a of Figure 8 and it was obtained with the CO molecule 4 Å above site "1". As it can be seen from comparison with the p-DOS of the clean metal surface shown in panel e, when the CO molecule is placed at 4 Å from the Au(321) surface, the bands due to the metal atoms are unchanged showing that there is not interaction. Upon adsorption on the most stable site on the Au(321) surface, i.e., above top "1", there is a visible shift of the CO bands (panel b in Figure 8) to more negative energies. Mainly, the chemical bond is the result of the overlap between the 5σ CO occupied orbital and the unoccupied $2\pi^*$ CO orbital with the gold states.[62-63] Nevertheless, as it is visible in panel b, there is also some overlap between the molecular orbital $1\ \pi$ of CO and the surface states. As a consequence, there is a broadening of the $2\pi^*$ (rightmost band in panel b), the shift of the 5σ band to more negative energies is larger than that of the $1\ \pi$ band and, consequently, the 5σ states appear on the left of the $1\ \pi$ states. Furthermore, the center of the d-band of the metal is also moved slightly to more negative energy. Globally, the picture is identical to that found for CO adsorbed on top sites of the Au(111) surface.[64]

In panels c and d of Figure 8, it is plotted the p-DOS for CO_2 positioned 4 Å above site "*1*" and at the optimal distance on the Au(321) surface, respectively. Since carbon dioxide interacts weakly with the gold surface under study, the p-DOS figures are almost the same for both cases. In fact, only a very light shift for more negative values is observed.

The p-DOS for CO and O species co-adsorbed on the Au(321) surface is shown in panel l of Figure 8. The p-DOS for the co-adsorbed CO and O species is identical to the sum of those obtained for an isolated oxygen atom adsorbed on a hollow site (panel i) and for CO adsorbed on a top site (panel b) and, hence, electronic changes due to cooperative co-adsorption seems to be absent in the most stable unreconstructed configuration optimized for CO and O on the Au(321) surface.

The evolution of the p-DOS along the oxidation of carbon monoxide by molecular oxygen starting from the four atom species adsorbed on the Au(321) surface is shown in panels f, g and h for OCOO initially adsorbed on $b_{1\text{-}2}$ and j, k and h for OCOO initially adsorbed on $b_{2\text{-}1}$, respectively. Similar but not identical p-DOS bands are obtained being the most important difference found for the oxygen states appearing at 5 eV. Nevertheless, albeit less noticeable, there are other important differences in the p-DOS upon the reaction of oxidation of CO by O_2. The proximity of several atoms in the case of the adsorbed OCOO four atoms species increases slightly the energy of the 2s states of the oxygen atom nearest to the surface. Furthermore, the center of the d-band is moved slightly to lower energies when the CO and O_2 molecules are close to each other, i.e., in the cases of the adsorbed OCOO species and also of the TS structure. This shows the role of the surface atoms in the oxidation reaction. Finally, in panel h, it is shown that the p-DOS for the products of the catalytic reaction, i.e., CO_2 and an adsorbed O atom, is similar to the sum of the p-DOS shown in panels d and i, respectively, for the separated CO_2 and O species adsorbed on the Au(321) surface.

4. Final remarks

The calculated energies of activation, E_a, for the reactions of dissociation of molecular oxygen,[49] and of CO oxidation by co-adsorbed atomic oxygen or molecular oxygen are the following:

$O_2^* \rightarrow 2\ O^*$ $\quad E_a \sim 1.0$ eV; (5)

$CO^* + O^* \rightarrow CO_2(g)$ $\quad E_a \sim 0.0$ eV; (6)

$CO^* + O_2^* \rightarrow CO_2(g) + O^*$ (via $OCOO^*$) $\quad E_a \sim 0.6$ eV, (7)

which lead to the subsequent conclusions. The reaction of oxygen dissociation on the Au(321) surface will be slow and, therefore, CO will initially be oxidized by molecular oxygen as described by reaction (7). The latter reaction generates O*, which makes reaction (6) viable. So, both oxidation reactions are important to the overall mechanism. Importantly, these low barriers for oxidation require various low-coordinated adsorption sites and strong reconstruction. In fact, the presence of low-coordinated Au atoms are associated with the surface reconstruction induced by the adsorbed species that seem to have an important role in the lower energy barriers for the surface reactions described above when compared with calculated data for surfaces where low-coordinated atoms are absent. Finally, we would like to emphasize that the surface model used in the present study resembles much closer the real catalysts since it includes a rather high heterogeneity of adsorption sites – surface positions in the middle of terraces, nearby kinks or steps – than other surfaces with lower Miller-indices.

5. Conclusions

The interaction of the CO, CO_2, CO+O and CO+O_2 with the Au(321) surface has been studied using a periodic supercell approach and carrying out spin polarized DFT calculations within the GGA/PW91 exchange-correlation functional.

Carbon monoxide is preferentially adsorbed, in C-down fashion, above the outermost surface atom and at the edges of the (111) terraces. The calculated adsorption energy on the kink sites is -0.77 eV and the distance of the carbon atom to the gold atom is 1.97 Å. The corresponding C-O bond length is 1.15 Å and this value increases up to 1.17 Å on positions where the interaction is weaker. Importantly, adsorption on bridge or hollow sites nearby the step is more favorable than adsorption on top of gold atoms in the middle of the terraces. In fact, bridge sites along the step are also very stable sites for CO adsorption. The preference for adsorption on the kink sites is still unchanged even in the presence of co-adsorbed atomic or molecular oxygen. Calculated co-adsorption energies are -1.03 eV and -0.76 eV, respectively.

The co-adsorption of a CO molecule and an oxygen atom on the unit cell used in this study leads to the formation of three highly stable structures. The calculated interaction energy for the most stable situation is -1.03 eV and it is the result of the

simultaneous interaction of the O atom and the CO molecule with the outermost atom on the surface which is the one with the lowest coordination. The strong interaction enlarges the distance between the outermost gold atom on the surface and the neighboring metal atoms. In the most stable configuration without surface deformation, carbon monoxide is adsorbed on the most favorable adsorption site refereed above and the oxygen atom is adsorbed on a hollow site in the middle of the terrace. The calculated co-adsorption energy is -0.72 eV.

The co-adsorption of CO and molecular oxygen yields three types of configurations on the Au(321) surface. These may be: separated co-adsorbed CO and molecular oxygen species; or, if they are placed at small distance, a four atoms compound adsorbed on the bridges forming the step or an adsorbed carbonate species appear upon the optimization procedure. The formation of these structures is thermodynamically favorable with respect to the energies of CO and O_2 in the gas-phase. The calculated interaction energy for adsorbed OCOO is -1.03 eV while for adsorbed CO_3 it is -3.53 eV.

The main product of the oxidation of CO, i.e., carbon dioxide, does not adsorb on the Au(321) surface since all tested configurations resulted in interaction energies of approximately zero eV.

The study of the reaction of CO oxidation by molecular or atomic oxygen on the Au(321) surface shows that the latter occurs almost without energy cost, in the regions nearby the step, on a reconstructed surface with an intercalated oxygen atom. Considering the final and initial positions for this reaction, the oxidation reaction is exothermic by -2.60 eV. The CO oxidation by direct reaction with molecular oxygen was studied using as initial states the OCOO compounds adsorbed on bridge sites nearby the step. Two very similar transition state structures were obtained with electronic energy barriers of 0.56 and 0.58 eV. Contrasting to previous results obtained for the dissociation of molecular oxygen on the same sites, the identical reaction barriers calculated for CO oxidation by molecular oxygen show that the reaction is equally favorable across the two bridges at the edges of the (111) terraces. Furthermore, it is suggested that the pre-dissociation of the molecular oxygen on the Au(321) surface for the CO oxidation is energetically less favorable than the direct reaction with molecular oxygen. The CO oxidation on the Au(321) surface by molecular oxygen is thermodynamic favorable by 2.41 eV when compared with the energy of the OCOO adsorbed species.

Finally, the present work supports the importance that low coordinated gold atoms, such as the outermost Au atom in the case of the Au(321) surface, have on the catalysis by gold surfaces, particles or thin-films.

Acknowledgments

Thanks are due to Fundação para a Ciência e Tecnologia (FCT), Lisbon, Portugal and to FEDER for financial support to CIQUP and to REQUIMTE. JLCF and JRBG acknowledge FCT for the grants with references, SFRH/BPD/27167/2006 and SFRH/BPD/24676/2005, respectively.

Supporting Information

Tables with geometric and energetic data for all studied configurations and Cartesian coordinates for selected configurations.

Figure 1. Possible adsorption sites on Au(321) surface, looking the surface from the top (a) or in the direction of the steps (b). *a*, *b*, *c*, *d*, *e*, *f*, *g*, *h* and *i* correspond to hollow positions and *1*, *2*, *3*, *4* and *5* to the top positions. The unit cell and the cell vectors are shown in (c).

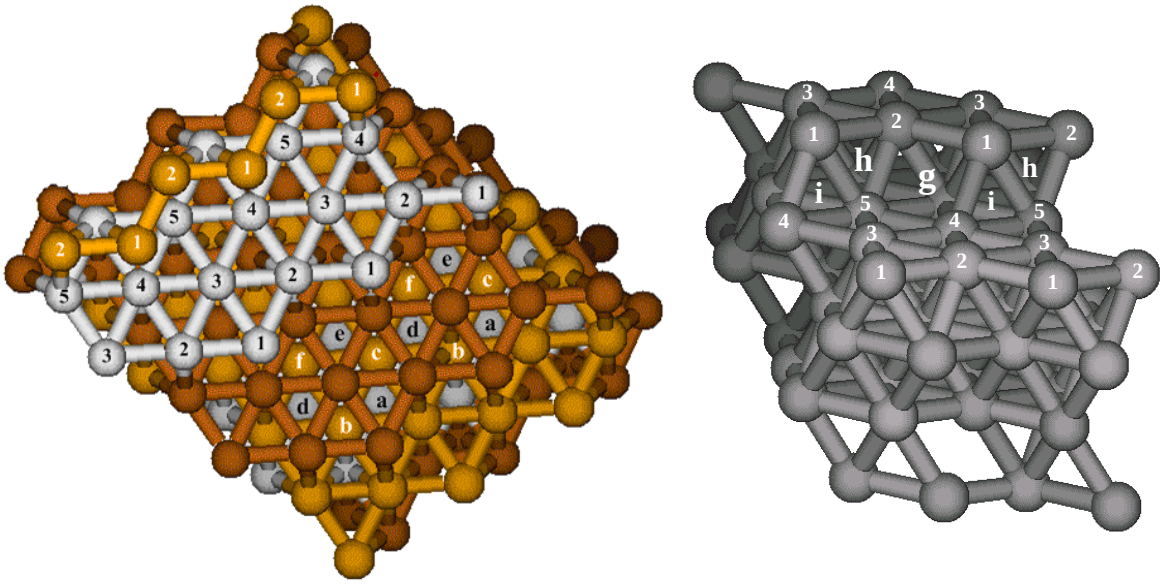

(a) (b)

(c)

Figure 2. Most stable adsorption positions for a) CO and b) CO_2 adsorbed on the Au(321) surface witch it is represented by the top layer. Interatomic distances are given in Å and several atoms were removed to turn the figures clearer.

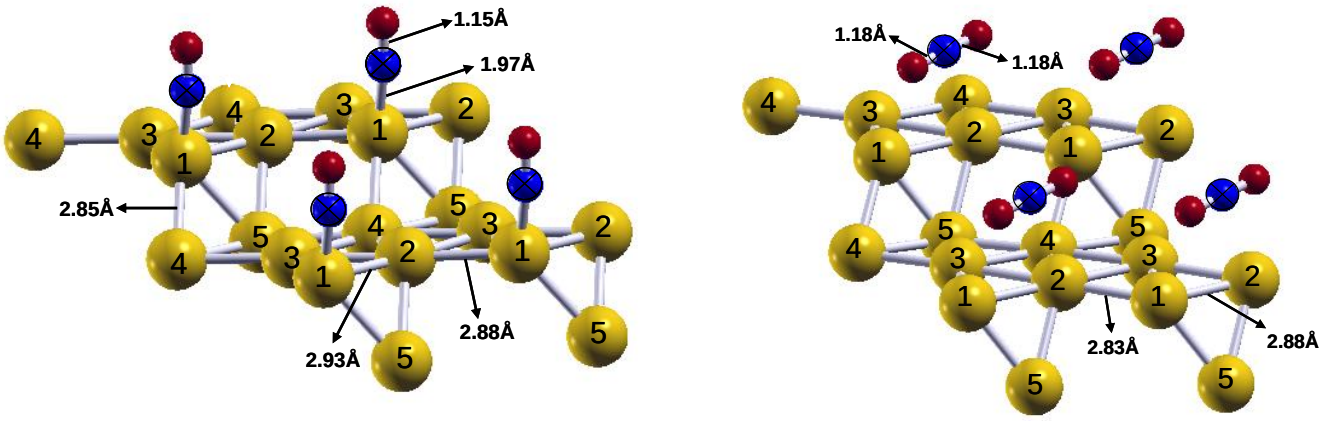

(a) (b)

Figure 3. Selected structures for co-adsorbed CO and O on the (a-c) reconstructed and (d) unreconstructed Au(321) surface. (a) shows a configuration with co-adsorbed species nearby atom *1* with the elongation of $b_{2\text{-}1}$ and $b_{4\text{-}1}$ while (b) and (c) show reconstructed configurations configurations with the co-adsorbed species nearby atom *1* with cleavage of $b_{4\text{-}1}$. Interatomic distances are given in Å and several atoms were removed to turn the figures clearer.

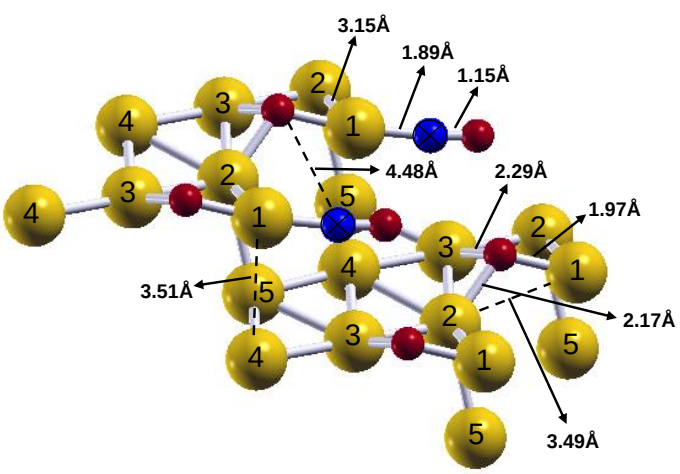

(a)

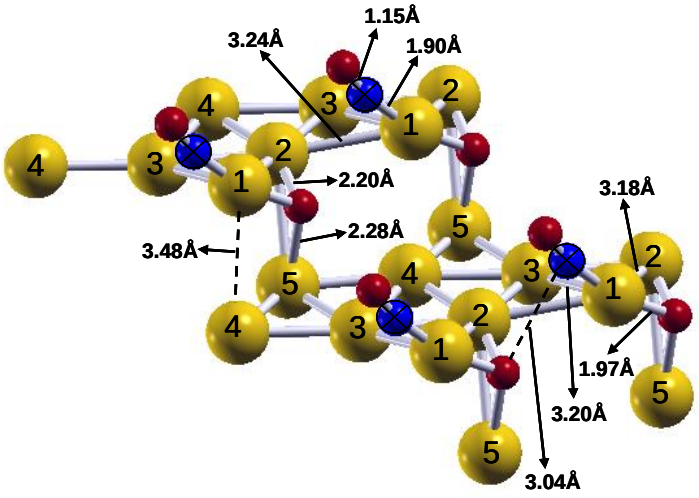

(b)

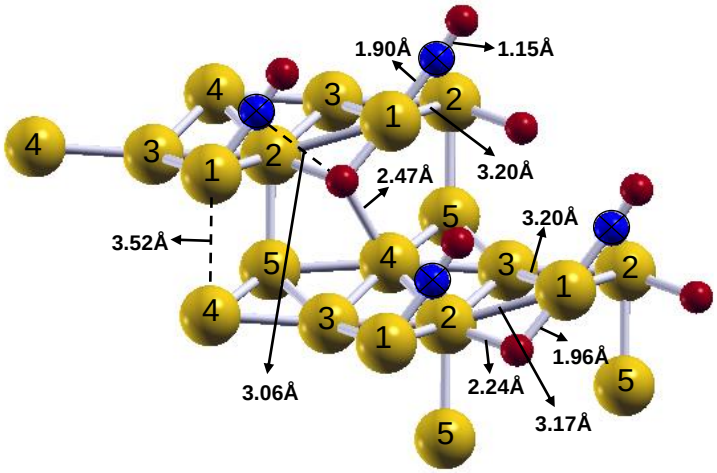

(c)

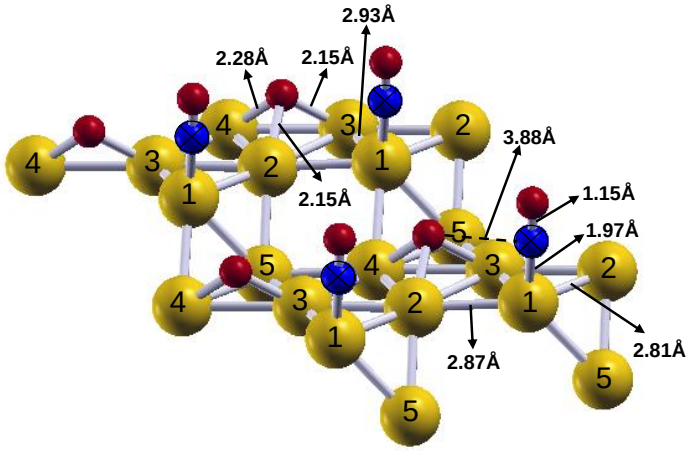

(d)

Figure 4. Selected structures for co-adsorbed CO and O_2 on the Au(321) surface. (a) four atoms OCOO compound adsorbed on $b_{2\text{-}1}$; (b) OCOO compound adsorbed on $b_{1\text{-}2}$ and (c) carbonate adsorbed on $b_{1\text{-}2}$. Interatomic distances are given in Å and several atoms were removed to turn the figures clearer.

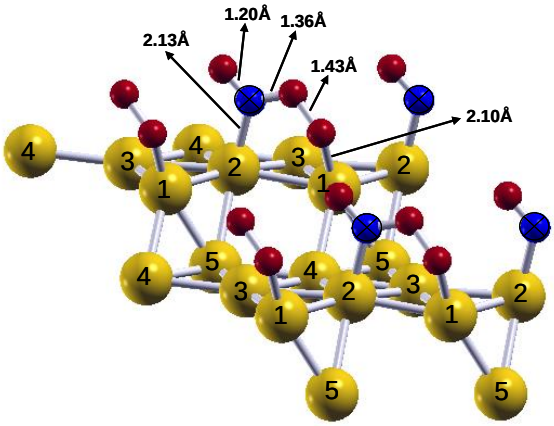

(a)

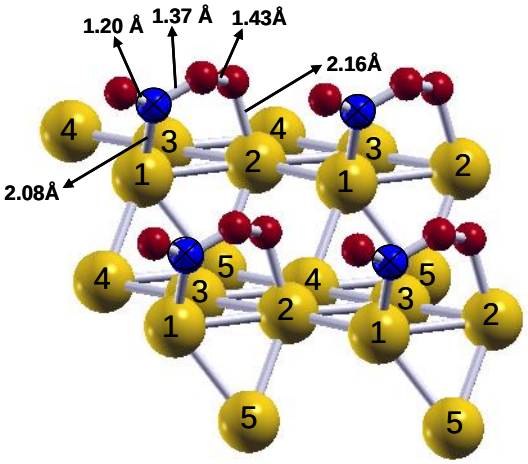

(b)

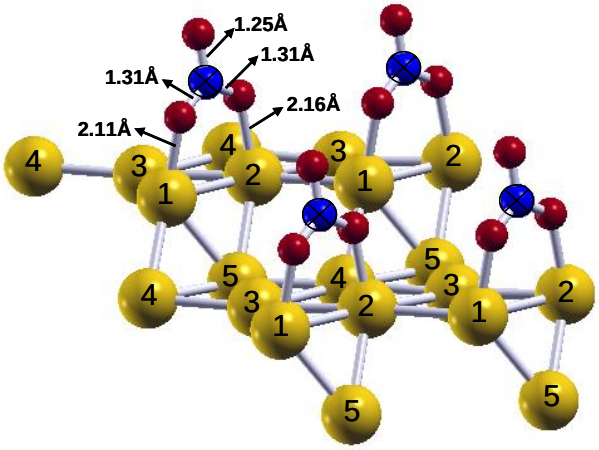

(c)

Figure 5. Transition state (TS) structures for the reaction between CO and O on the Au(321) surface. (a) - (d) illustrate the TS structures obtained from the starting configurations shown in Figs. 3a - 3d, respectively. Interatomic distances are given in Å and several atoms were removed to turn the figures clearer.

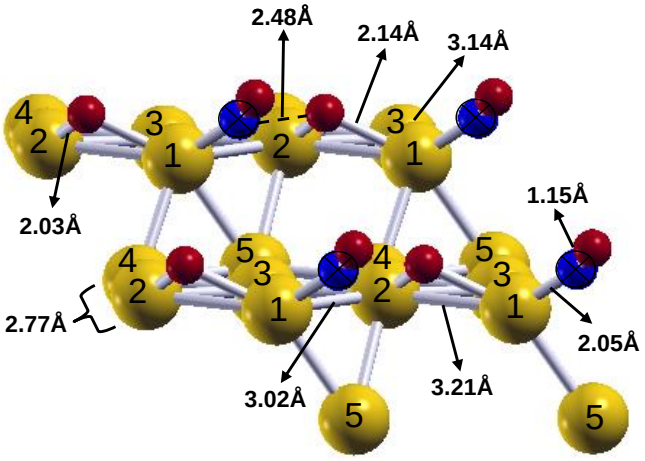

(a)

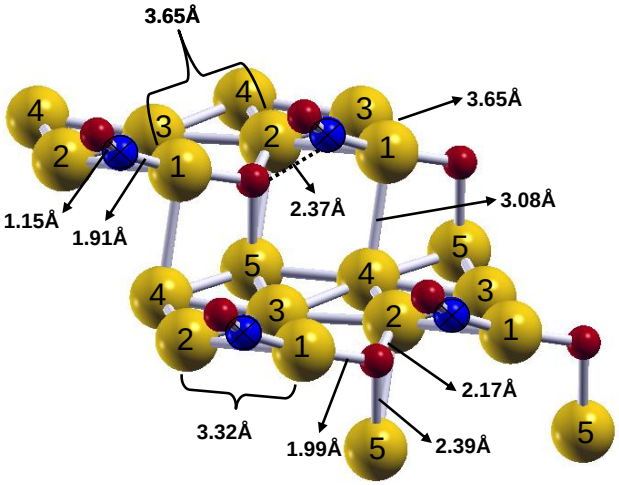

(b)

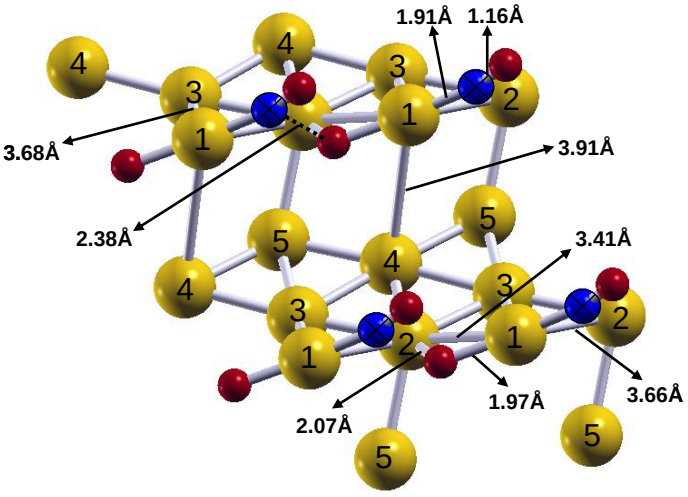

(c)

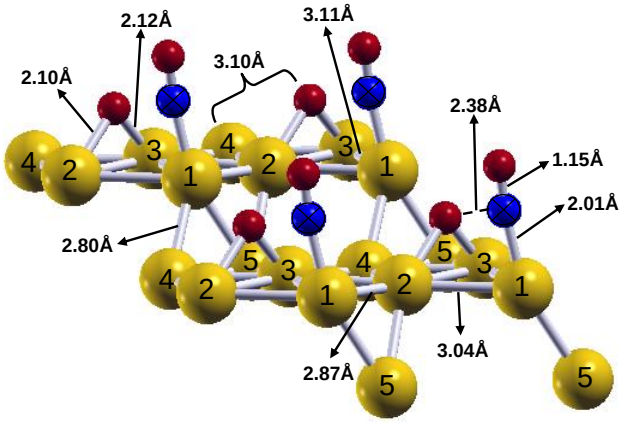

(d)

Figure 6. Transition state (TS) structures for the OCOO → CO_2 + O reaction on the Au(321) surface starting from the initial OCOO compound adsorbed on $b_{2\text{-}1}$ (a) on $b_{1\text{-}2}$ (b). The final state for the OCOO dissociation is shown in (c). Interatomic distances are given in Å and several atoms were removed to turn the figures clearer.

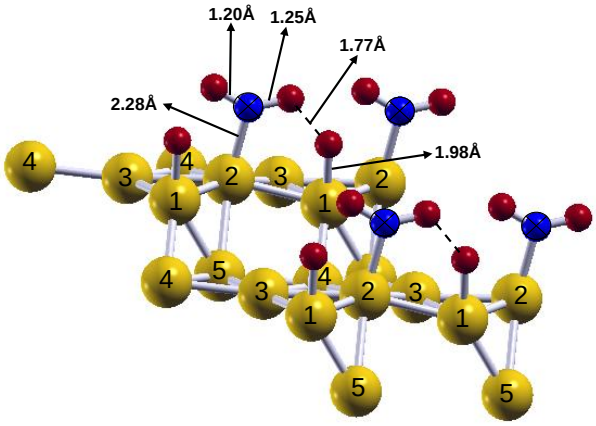

(a)

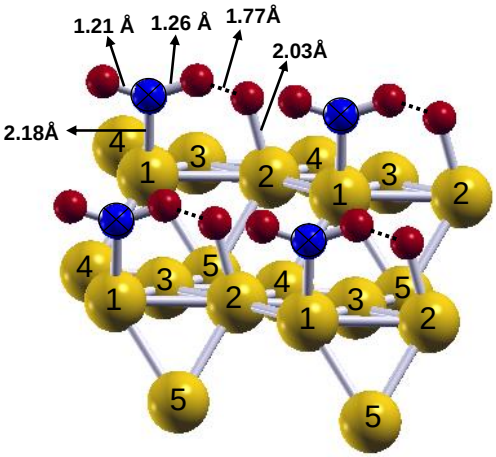

(b)

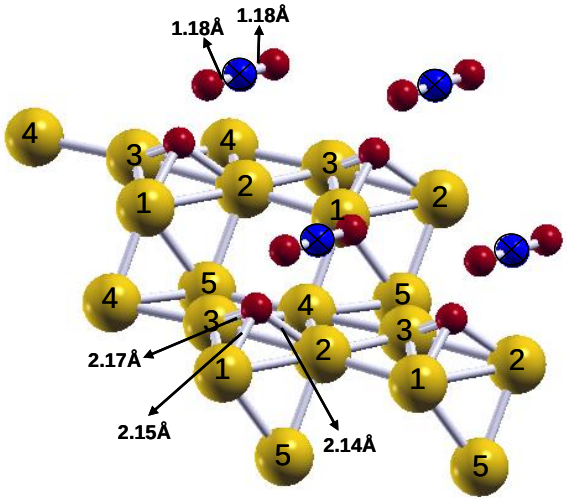

(c)

Figure 7. Reaction profile for the CO oxidation by direct reaction with molecular oxygen on the $b_{2\text{-}1}$ site. The variation of the energy (eV) and the C-O and O-O distances (Å) during the process are included. IS, TS and FS stand for the initial, transition and final states, respectively. Red(dark), white(clear) and yellow(grey) balls are used for oxygen, carbon and gold atoms, respectively.

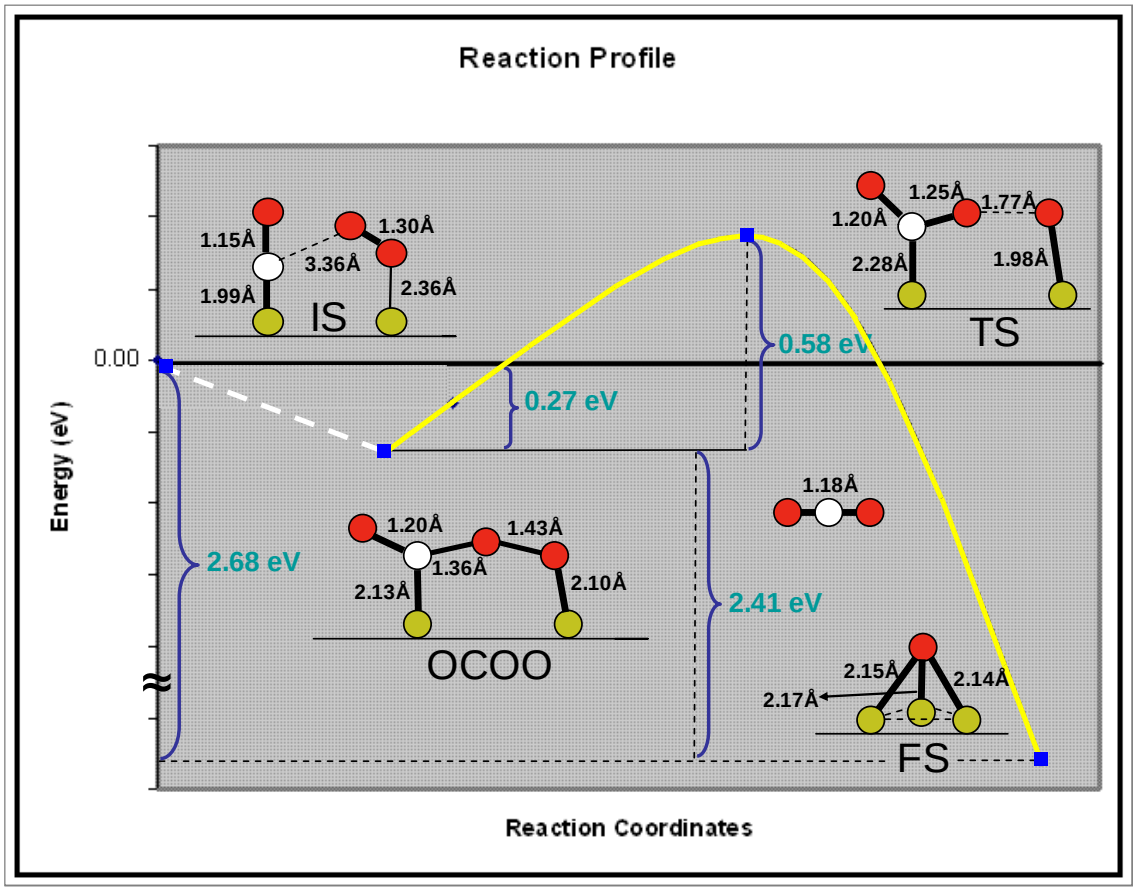

Figure 8. Density of states for: **a**) free CO molecule; **b**) CO adsorbed on top "1"; **c**) free CO_2 molecule; **d**) CO_2 interacting with the Au(321) surface; **e**) clean Au (321) surface; **f**) four atoms compound on $b_{1\text{-}2}$; **g**) transition state along $b_{1\text{-}2}$; **h**) final state; **i**) an oxygen atom adsorbed on hole "a"; **j**) four atoms compound on $b_{2\text{-}1}$; **k**) transition state along $b_{2\text{-}1}$; and **l**) CO + O co-adsoportion. In panel **e,** dotted, dashed and solid lines represent the metal *s*, *p* and *d* states, respectively while in the rest of the panels, dotted line represents the gold states (s,p,d), dashed line represents the carbon states (s,p) and solid line represents the oxygen states (s,p). Only the states of the two outermost gold atoms, those forming the zig-zag step are considered. Arbitrary units are used for Y axis.

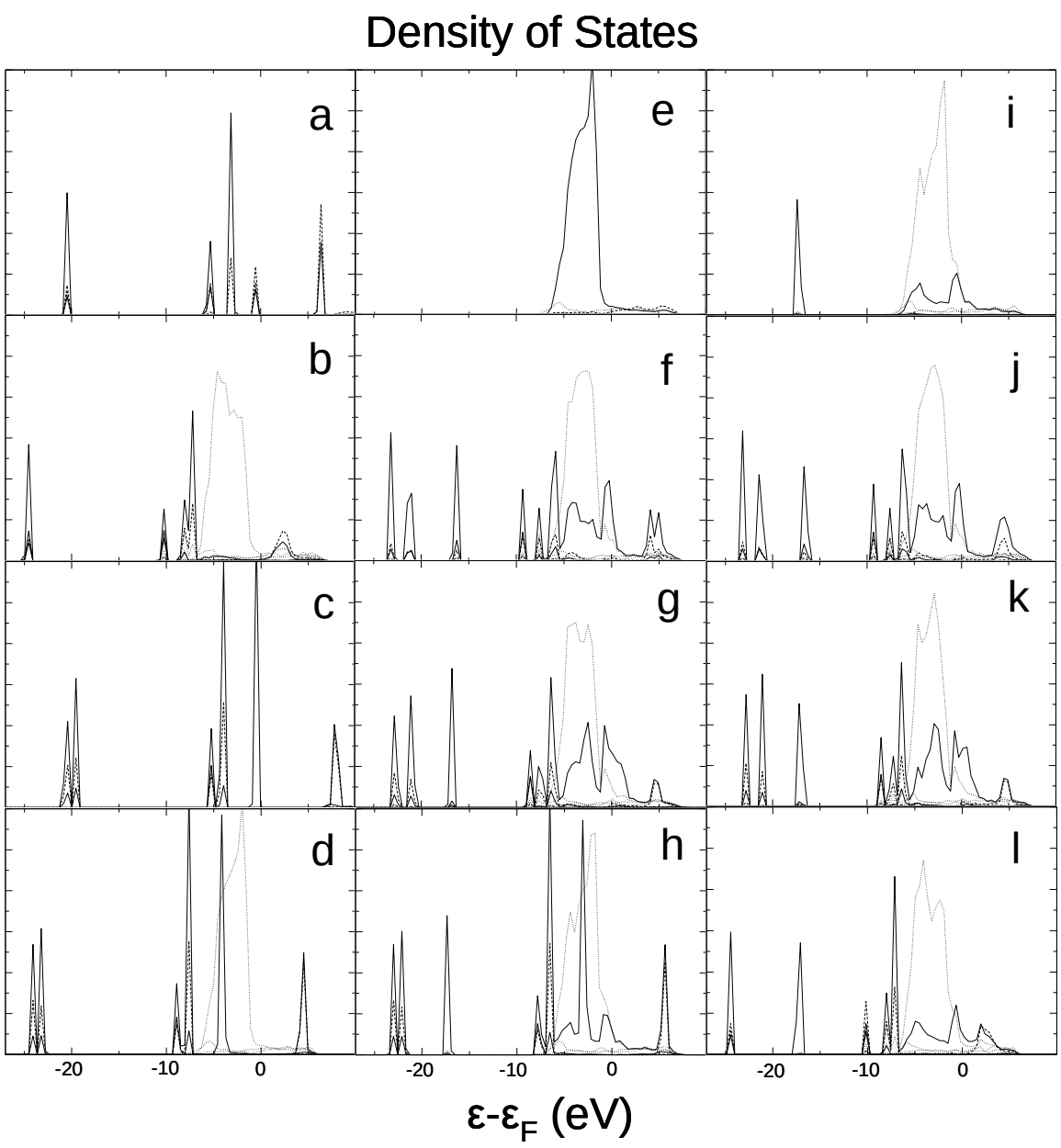

Table 1. Most favorable adsorption energies (eV) and distances (Å) between the carbon atom (the oxygen atom) and nearest-neighbor gold atoms for CO adsorbed on the Au(321) surface.[a]

Adsorption on surface cavities			Adsorption directly above Au atoms		
Position	E_{ads}	C-Au distances	Position	E_{ads}	C-Au distance
hole "*a*"	-0.49	2.14 (*1*); 2.13(*2*); 2.90(*3*)	top "*1*"	-0.77	1.97(*1*)
hole "*b*"	-0.53	2.14(*1*); 2.12(*2*); 3.07(*3*)	top "*2*"	-0.42	2.00(*2*)
hole "*g*"	-0.49	2.11(*1*); 2.17(*2*); 3.56(*4*); 3.63*(5)*			
Adsorption on surface bridges					
Position	E_{ads}	C-Au distances	Position	E_{ads}	C-Au distances
$b_{1\text{-}2}$	-0.60	2.12(*1*); 2.13(*2*)	$b_{2\text{-}1}$	-0.61	2.12(*1*); 2.12(*2*)

[a] Numbers in italic and inside parenthesis are labels for surface gold atoms, *c.f.*, Figure 1. The CO distance is 1.15 Å for the adsorption on *top* and 1.17 Å for the adsorption on *bridge* and *hole* sites.

Table 2. Most favorable coadsorption energies (eV) and distances (Å) between carbon and oxygen atoms (atomic oxygen) to the nearest gold atom for CO+O co-adsorption on the Au(321) surface.[a]

Position[b] O-CO	E_{coads}	Distances[c] O-Au; C-Au
hole "*b*"- top "*1*"	-1.03	1.97(*1*); 1.89(*1*)[d]
hole "*h*"- top "*1*"	-0.84	1.97(*1*); 1.90(*1*)[e]
hole "*g*"- top "*1*"	-0.82	1.96(*1*); 1.90(*1*)[f]
hole "*d*"- top "*1*"	-0.72	2.15(*2*); 1.96(*1*)[g]

[a]Numbers in italic and inside parenthesis are labels for surface gold atoms, *c.f.*, Figure 1. The CO distance is ~ 1.15 Å for all the adsorptions on *top* and between 1.16-1.17 for the adsorption on *bridge* and *top* sites.

[b] The notation is as follows: the first term corresponds to the position of the oxygen atom (atomic oxygen) and the second term corresponds to the position of the carbon atom.

[c] Distances from the carbon and oxygen (atomic oxygen) atoms to the nearest gold atom.

[d] This structure is shown in Figure 3a.

[e] This structure is shown in Figure 3b.

[f] This structure is shown in Figure 3c.

[g] This structure is shown in Figure 3d.

Table 3. Most favorable coadsorption energies (eV) and distances (Å) for $CO+O_2$ co-adsorption on the Au(321) surface.[a]

Position[b] O_a-O_b	CO	$E_{co\text{-}ads}$	Distances[c] O-O; O_a-Au; O_b-Au	Distances[d] C-O; C-$Au_{1\text{-}2}$
top "*2*"- $b_{3\text{-}2}$	top "*1*"	-0.76	1.30; 2.36(*2*); 2.68(*3*)	1.15; 1.99(*1*)
$b_{2\text{-}3}$	top "*1*"	-0.73	1.26; 3.16(*2*); 2.83(*3*)	1.15; 1.99(*1*)
top "*1*"- $b_{4\text{-}3}$	top "*2*"	-0.63	1.29; 2.31(*1*); 2.77(*3*)	1.15; 2.01(*2*)
top "*1*"- $b_{1\text{-}2}$	top "*2*"	-0.64	1.30; 2.20(*1*); 3.06(*1*)	1.16; 2.10(*2*)
top "*1*"- step	top "*2*"	-0.63	1.27; 2.30(*1*); 3.10(*1*)	1.15; 2.02(*2*)
top "*2*"- $b_{2\text{-}1}$	top "*1*"	-0.66	1.28; 2.36(*2*); 3.60(*1*)	1.15; 1.97(*1*)
OCOO compound on $b_{1\text{-}2}$		-1.01	$d_{C\text{-}Au(1)}$= 2.08; $d_{O\text{-}Au(2)}$= 2.16[e]	
OCOO compound on $b_{2\text{-}1}$		-1.03	$d_{C\text{-}Au(2)}$= 2.13; $d_{O\text{-}Au(1)}$= 2.10[e]	
Carbonate on $b_{1\text{-}2}$		-3.53	$d_{O\text{-}Au(1)}$= 2.11; $d_{O\text{-}Au(2)}$= 2.16[e]	

[a]Numbers in italic and inside parenthesis are labels for surface gold atoms, *c.f.*, Figure 1.

[b] The notation is as follows: the terms in the first column correspond to the atomic positions of the oxygen molecule while those in the second column correspond to the position of the carbon atom of C-down carbon monoxide.

[c] Interatomic distance in molecular oxygen and distances between oxygen and nearest gold atoms.

[d] Interatomic distance in CO and distances between carbon and nearest gold atoms.

[e] These structures are shown in Figure 4a (OCOO on $b_{2\text{-}1}$), Figure 4b (OCOO on $b_{1\text{-}2}$) and Figure 4c (carbonate).

References

1 Haruta, M.; Yamada, N.; Kobayashi, T.; Iijima. S. *J. Catal.* **1989**, 115, 301.

2 Qian, L. H.; Wang, K.; Li, Y.; Fang, H. T.; Lu, Q. H.; Ma, X. L. *Mater. Chem. Phys*. **2006**, 100, 82.

3 Matsuoka, K.; Miyazaki, K.; Iriyama, Y.; Kikuchi, K.; Abe, T.; Ogumi, Z. *J. Phys. Chem. C* **2007**, 111, 3171.

4 Kim, H.-J.; Kim, D.-Y.; Han, H.; Shul, Y.-G. *J. Power Sources* **2006**, 159, 484.

5 Pestryakov, A. N.; Bogdanchikova, N.; Simakov, A.; Tuzovskaya, I.; Jentoft, F.; Farias, M.; Díaz, A. *Surf. Sci*. **2007**, *601*, 3792.

6 Sanchez-Castillo, M.A.; Couto, C.; Kim, W.B.; Dumesic, J.A. *Angew. Chem. Int. Ed.*, **2004**, *43*, 1140.

7 Xu, C.; Su, J.; Xu, X.; Liu, P.; Zhao, H.; Tian, F.; Ding, Y. *J. Am. Chem. Soc*. **2007**, 129, 42.

8 Zielasek, V.; Jurgens, B.; Schulz, C.; Biener, J.; Biener, M. M.; Hamza, A. V.; Bäumer, M.; *Angew. Chem. Int. Ed.* **2006**, *45*, 8241.

9 Xu, C.; Xu, X.; Su, J.; Ding, Y.; *J. Catal.* **2007**, *252*, 243.

10 Chen, M.; Goodman, D. W. *Acc. Chem. Res*. **2006**, 39, 739.

11 Schubert, M. M.; Hackenberg, S.; van Ween, A. C.; Muhler, M.; Plzak, V.; Behm, R. J. *J. Catal.* **2001**, 197, 113.

12 Grzybowska-Świerkosz, B. *Catal. Today* **2006**, 112, 3.

13 Comotti, M.; Li, W.-C.; Spliethoff, B.; Schüth, F. J. Am. Chem. Soc. **2006**, 128, 917.

14 Lopez, N.; Janssens, T. V. W.; Clausen, B. S.; Xu, Y.; Mavrikakis, M.; Bligaard, T.; Nørskov, J. K. *J. Catal.* **2004**, 223, 232.

15 Remediakis, I. N.; López, N.; Nørskov, J. K. *App. Catal. A: General* **2005**, 291, 13.

16 Moreau, F.; Bond, G. C. *Catal. Today* **2007**, 122, 215.

17 Janssens, T. V. W.; Carlsson, A.; Puig-Molina, A.; Clausen, B. S. *J. Catal.* **2006**, 240, 108.

18 Guzman, J.; Carrettin, S.; Corma, A. *J. Am. Chem. Soc.* **2005**, 127, 3286.

19 Wang, C.-M.; Fan, K. –N.; Liu, Z. –P. *J. Am. Chem. Soc.* **2007**, 129, 2642.

20 Pala, R. G. S.; Liu, F. *J. Chem. Phys.* **2006**, 125, 144714.

21 Arenz, M.; Landman, U.; Heiz, U. ChemPhysChem **2006**, 7, 1871.

22 Mavrikakis, M.; Stoltze, P.; Nørskov, J. K. *Catal. Lett*. **2000**, 64, 101.

23 Xu, Y.; Mavrikakis, M. *J. Phys. Chem*. B **2003**, 107, 9298.

24 Daté, M.; Imai, H.; Tsubota, S.; Haruta, M. *Catal. Today* **2007,** 122, 222.

25 Zou, X. –H.; Qi, S. –X.; Suo, Z. –H.; An, L. –D.; Li, F. *Catal. Commun.* **2007**, 8, 784.

26 Clark, J. C.; Dai, S.; Overbury, S. H. *Catal. Today* **2007**, 126, 135.

27 Burch, R. *Phys. Chem. Chem. Phys.* **2006**, 8, 5483.

28 Zhang, X.; Shi, H.; Xu, B. –Q. *Catal. Today* **2007**, 122, 330.

29 Wang, S.; Zhao, Y.; Huang, J.; Wang, Y.; Ren, H.; Wu, S.; Zhang, S.; Huang, W. *App. Surf. Sci.* **2007**, 253, 3057.

30 Ma, Z.; Brown, S.; Overbury, S. H.; Dai, S. *App. Catal. A: General* **2007**, 327, 226.

31 Weiher, N.; Beesley, A. M.; Tsapatsaris, N.; Delannoy, L.; Louis, C.; van Bokhoven, J. A.; Schroeder, S. L. M. *J. Am. Chem. Soc.* **2007**, 129, 2240.

32 Hickey, N.; Larochette, P. A.; Gentilini, C.; Sordelli, L.; Olivi, L.; Polizzi, S.; Montini, T.; Fornasiero, P.; Pascuato, L.; Graziani, M. *Chem. Mater*. **2007**, 19, 650.

33 Steyn, J.; Pattrick, G.; Scurrell, M. S.; Hildebrandt, D.; Raphulu, M. C.; van der Lingen, E. *Catal. Today* **2007**, 122, 254.

34 Szabó, E. G.; Tompos, A.; Hegedűs, M.; Szegedi, Á.; Margitfalvi, J. L. *App. Catal. A: General* **2007**, 320, 114.

35 Romero-Sarria, F.; Martínez T., L. M.; Centeno, M. A.; Odriozola, J. A. *J. Phys. Chem. C*, **2007**, 111, 14469.

36 Manzoli, M.; Boccuzzi, F.; Chiorino, A.; Vindigni, F.; Deng, W.; Flytzani-Stephanopoulus, M. *J. Catal.* **2007**, 245, 308.

37 Fierro-Gonzalez, J. C.; Gates, B. C. *Catal. Today* **2007**, 122, 201.

38 Fu, L.; Wu, N. Q.; Yang, J. H.; Qu, F.; Johnson, D. L.; Kung, M. C.; Kung, H. H.; Dravid, V. P. *J. Phys. Chem. B* **2005**, 109, 3704.

39 Gluhoi, A. C.; Nieuwenhuys, B. E. *Catal. Today* **2007**, 122, 226.

40 Sadek, M. M.; Wang, L. *J. Phys. Chem. A* **2006** 110, 14036.

41 Vassilev, P.; Koper, M. T. M. *J. Phys. Chem. C* **2007**, jp064515.

42 Liu, Z. –P.; Hu, P.; Alavi, A. *J. Am. Chem. Soc*. **2002**, 124, 14770.

43 Lopez, N.; Nørskov, J. K. *J. Am. Chem. Soc.* **2002**,124, 11262.

44 Wang, Y.; Gong, X. G.; *J. Chem. Phys*. **2006**, 125, 124703.

45 Lim, D. C.; Lopez-Salido, I.; Dietsche, R.; Bubek, M.; Kim, Y. D. *Angew. Chem. Int. Ed.* **2006**, 45, 2413.

46 Lim, D. C.; Lopez-Salido, I.; Dietsche, R.; Bubek, M.; Kim, Y. D. *Surf. Sci.* **2006**, 600, 507.

47 Min, B. K.; Alemozafar, A. R.; Pinnaduwage, D.; Deng, X.; Friend, C. M. *J. Phys. Chem. B* **2006**, 110, 19833.

48 Fajin, J. L. C.; Cordeiro, M. N. D. S.; Gomes, J. R. B., *Surf. Sci*, **2008**, 602, 424.

49 Fajin, J. L. C.; Cordeiro, M. N. D. S.; Gomes, J. R. B. *J. Phys. Chem. C.* **2007**, *111*, 17311.

50 Kung, M. C.; Davis, R. J.; Kung, H. H. *J. Phys. Chem. C* **2007**, 111, 11767.

51 Kresse, G. ; Hafner, J. *Phys. Rev. B* **1993**, 47, 558.; Kresse, G.; Furthmüller, J. *Comput. Mater. Sci.* **1996**, 6, 15.; Kresse, G.; Furthmüller, J. *Phys. Rev. B* **1996**, 54, 11169.

52 Perdew, J. P.; Chevary, J. A.; Vosko, S. H.; Jackson, K. A.; Pederson, M. R.; Singh, D. J.; Fiolhais, C. *Phys. Rev. B* **1992**, 46, 6671.

53 Blöchl, P. E. *Phys. Rev. B* **1994**, 50, 17953.

54 Kresse, G.; Joubert, D. *Phys. Rev. B* **1999**, 59, 1758.

55 Jónsson, H.; Mills, G.; Jacobsen, K. W. In *Classical and Quantum Dynamics in Condensed Phase Simulations*; Berne, B. J.; Ciccotti, G.; Coker, D. F. Eds.; *World Scientific: Singapore*, **1998**; p 385.

56 Henkelman, G.; Jónsson, H. *J. Chem. Phys*. **2000**, 113, 9978.

57 Henkelman, G.; Jónsson, H. *J. Chem. Phys*. **1999**, 111, 7010.

58 Pacchioni, G. *Surf. Sci.* **2002**, 520, 3.

59 McFadden, C. F.; Cremer, P. S.; Gellman, A. J. *Langmuir* **1996**, 12, 2483.

60 Stiehl, J. D.; Gong, J.; Ojifinni, R. A.; Kim, T. S.; McClure, S. M.; Mullins, C. B. *J. Phys. Chem. B* **2006**, 110, 20337.

61 Westerström, R.; Wang, J. G.; Ackermann, M. D.; Gustafson, J.; Resta, A.; Mikkelsen, A.; Andersen, J. N.; Lundgren, E.; Balmes, O.; Torrelles, X.; Frenken, J. W. M.; Hammer, B. J. Phys.: Condens. Matter, **2008**, 20, 184018.

62 Chen, Y.-H.; Cao, D.-B.; Jun, Y.; Li, Y.-W.; Wang, J.; Jiao, H. *Chem. Phys. Lett.* **2004**, 400, 35.

63 Sung, S. S.; Hoffmann, R. *J. Am. Chem. Soc.* **1985**, 107, 578.

64 Gajdoš, M.; Eichler, A.; Hafner, J. *J. Phys.: Condens. Matter* **2004**, 16, 1141.